Supplement of Geosci. Model Dev., 18, 4899–4913, 2025
https://doi.org/10.5194/gmd-18-4899-2025-supplement

Geoscientific Model Development
Open Access
EGU

Supplement of

Assessing modifications to the Abdul-Razzak and Ghan aerosol activation parameterization (version ARG2000) to improve simulated aerosol–cloud radiative effects in the UK Met Office Unified Model (UM version 13.0)

Pratapaditya Ghosh et al.

Correspondence to: Hamish Gordon (gordon@cmu.edu)

Table S1. Aerosol concentrations and geometric mean diameters used to prepare the supplementary figures. The first three columns represent number concentrations in Aitken, accumulation and coarse mode. The last three columns represent geometric mean diameter of Aitken, accumulation, and coarse mode. Hygroscopicity, pressure and temperature are kept fixed at 0.6, 101325 Pa, and 20°C for all the plots except Figure S4, where the dependence of the activation fraction on hygroscopicity, temperature, and pressure is shown.

Figure	N_{ait} (cm^{-3})	N_{acc} (cm^{-3})	N_{coa} (cm^{-3})	D_{ait} (nm)	D_{acc} (nm)	D_{coa} (nm)
S1	40	200	5	40	200	800
S3: Top	50	4000	5	40	150	800
S3: Middle	500	200	5	40	100	800
S3: Bottom	5000	200	5	70	100	800
S4	50	200	5	40	100	800
S5	50	100	5	40	100	800
S6: Top	50	4000	5	40	150	800
S6: Middle	500	100	5	40	150	800
S6: Bottom	50	200	0.5	40	150	800
S14: Top	50	150	5	40	100	800
S14: Bottom	50	300	5	40	200	800

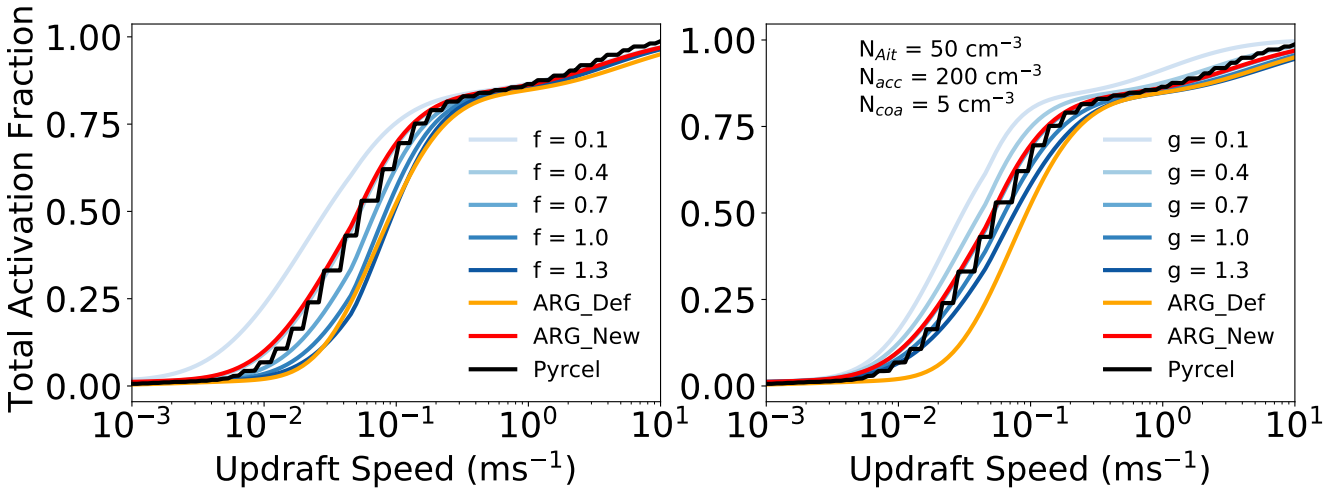

Figure S1. Total activation fraction (with $\sigma_{acc} = 1.4$) as a function of updraft speed for different values of f (left panel) and g (right panel). On the left, we used $g = 0.67$ in line with Equation 5 in the main text, while varying f from 0.1 to 1.3. On the right, we used $f = 0.37$ in line with Equation 5 in the main text while varying g from 0.1 to 1.3. The performance of the default and updated ARG is also shown and compared with the parcel model. The accumulation mode aerosol number concentration is 200 cm^{-3}; other details are given in Table S1. In the equations of Abdul-Razzak and Ghan (2000), labelled as ARG_Def, $f_{acc} = 0.66$, $g_{acc} = 1.08$ and $p = 1.50$ for $\sigma_{acc} = 1.4$. In the updated version labelled as ARG_New, we recommend $f = 0.37$, $g = 0.67$ and $p = 0.88$ (for kinetically limited cases) for $\sigma_{acc} = 1.4$ in all the aerosol modes.

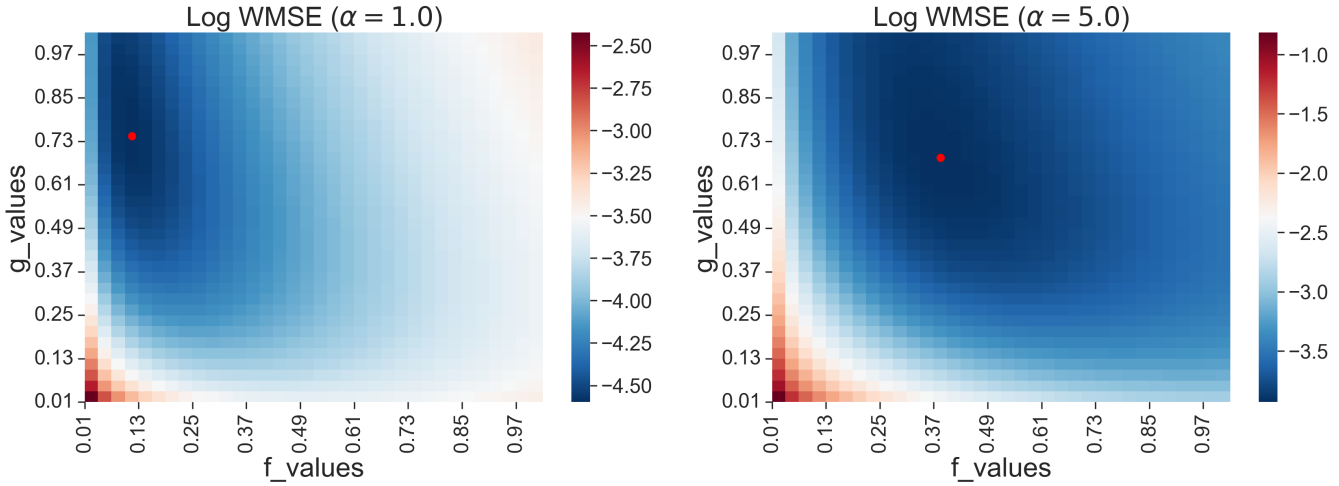

Figure S2. The logarithm of the Weighted Mean Squared Error (WMSE) value of the activation fraction in the comparison of the updated ARG to the parcel model as a function of f and g. The left panel is for asymmetry factor $\alpha = 1.0$, and the right panel is for asymmetry factor $\alpha = 5.0$. The accumulation mode geometric standard deviation is 1.4. In this paper, we use $\alpha = 5.0$. In the left panel, with $\alpha = 1.0$, WMSE is equivalent to the Mean Squared Error (MSE). All Pyrcel simulations for which kinetic limitations are not important are used to calculate the WMSE values. The red dots denote the location of minimum WMSE.

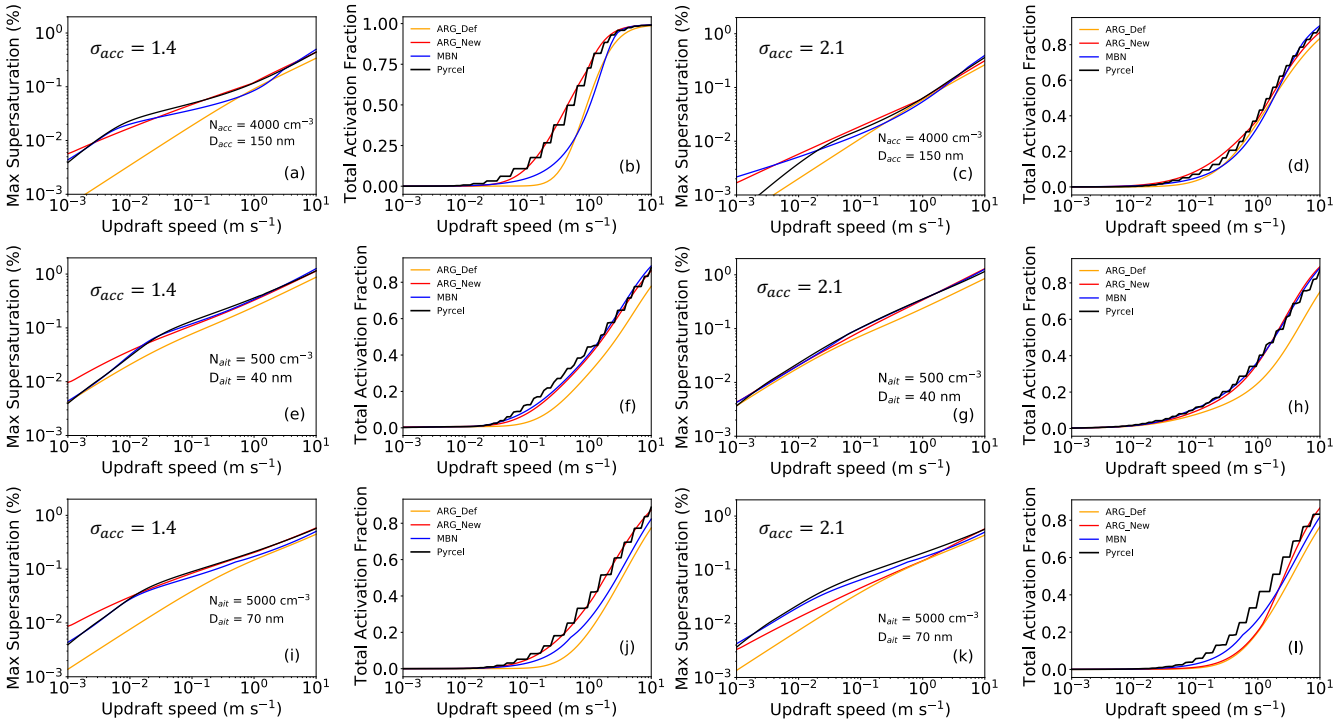

Figure S3. Maximum supersaturations and total aerosol activation fractions for different accumulation and Aitken mode aerosol number concentrations and geometric mean diameters compared with the parcel model for $\sigma_{acc} = 1.4$ (left panels) and $\sigma_{acc} = 2.1$ (right panels). Details of the aerosol size distributions are in Table S1.

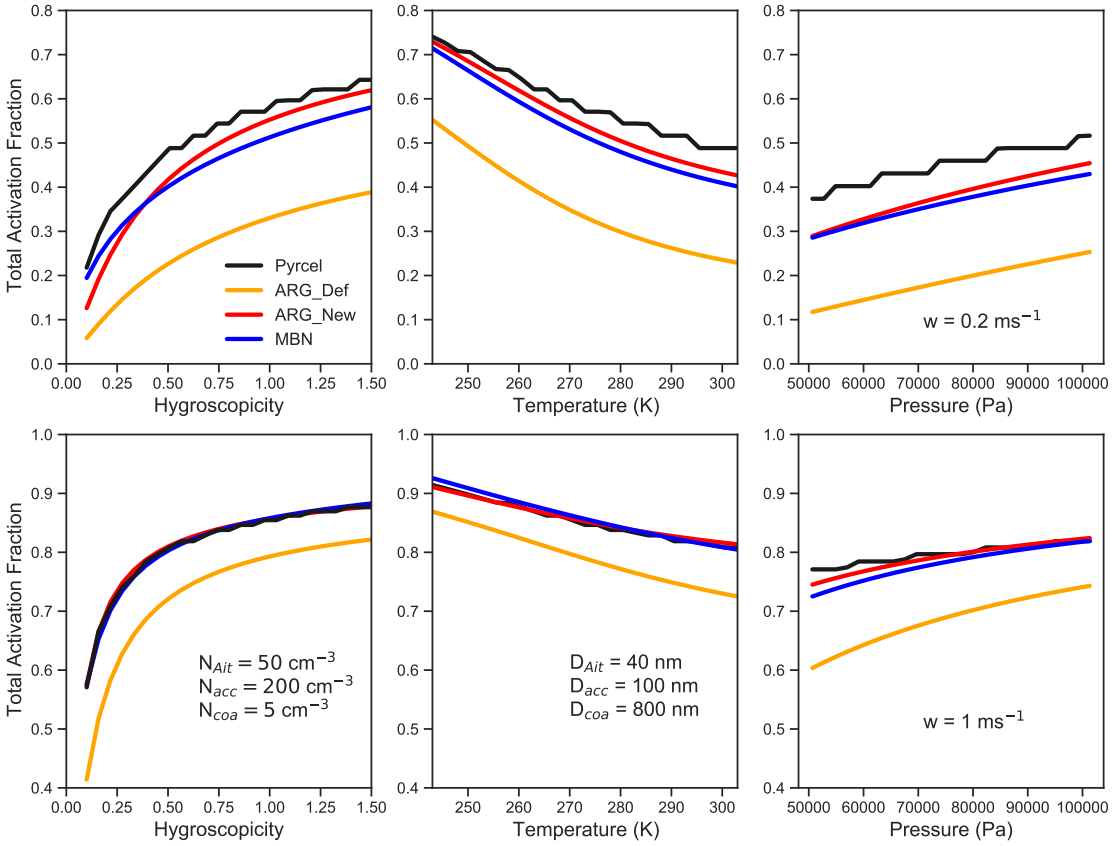

Figure S4. From left to right: total activation fraction as a function of hygroscopicity (κ), temperature and pressure for the updraft speed 0.2 ms^{-1} (top panel) and 1 ms^{-1} (bottom panel). We used simulations with 100 cm^{-3} accumulation mode aerosols ($\sigma_{acc} = 1.4$) to prepare this figure. Other details are given in Table S1.

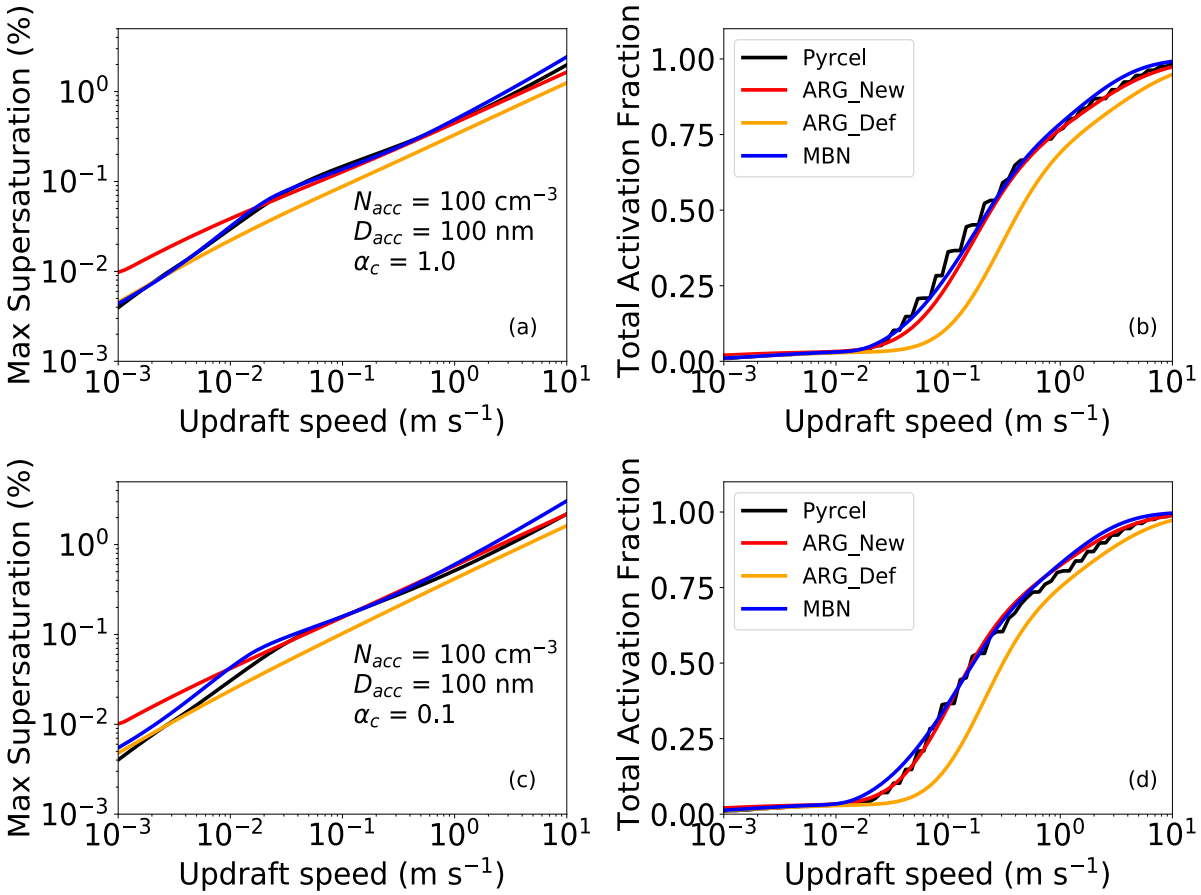

Figure S5. Sensitivity of results to mass accommodation coefficient α_c. The figure shows the maximum supersaturation (subfigure a, c) and total activation fraction (subfigure b, d) from the default ARG scheme, new ARG scheme, MBN scheme and the parcel model, as a function of updraft velocities, for two different α_c. We used simulations with 100 cm^{-3} accumulation mode aerosols and $\sigma_{acc} = 1.4$; other details are listed in Table S1. For $\alpha_c = 1.0$, the mean bias in activation fraction for default and new ARG is -7.7% and -1.5%. For $\alpha_c = 0.1$, the mean bias in activation fraction for default and new ARG is -5.8% and 0.9% (for the conditions in this figure, not for the entire parameter space).

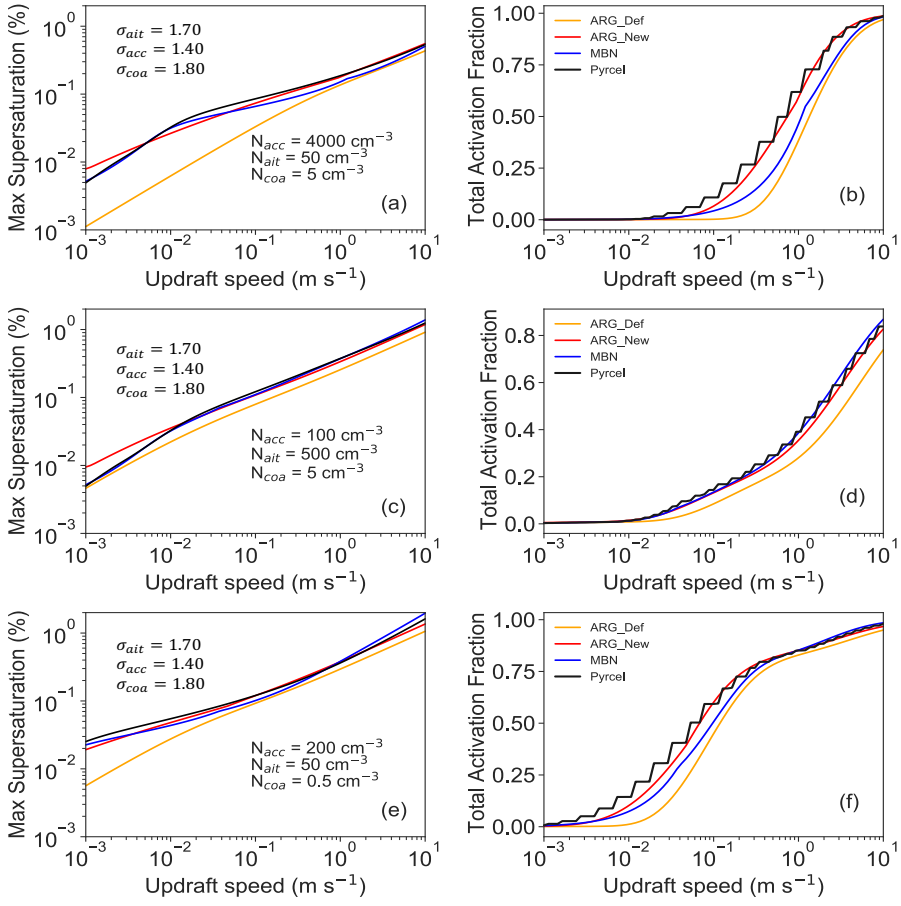

Figure S6. Maximum supersaturations and total aerosol activation fractions for different Aitken, accumulation and coarse mode aerosol number concentrations compared with the parcel model. Here, the widths of the Aitken, accumulation, and coarse modes aare kept fixed at 1.7, 1.4, and 1.8 instead of the usual 1.6, 1.4, 2.0. The geometric mean diameter of Aitken, accumulation, and coarse mode aerosols are kept fixed at 40 nm, 150 nm, and 800 nm. Details of the aerosol size distributions are in Table S1.

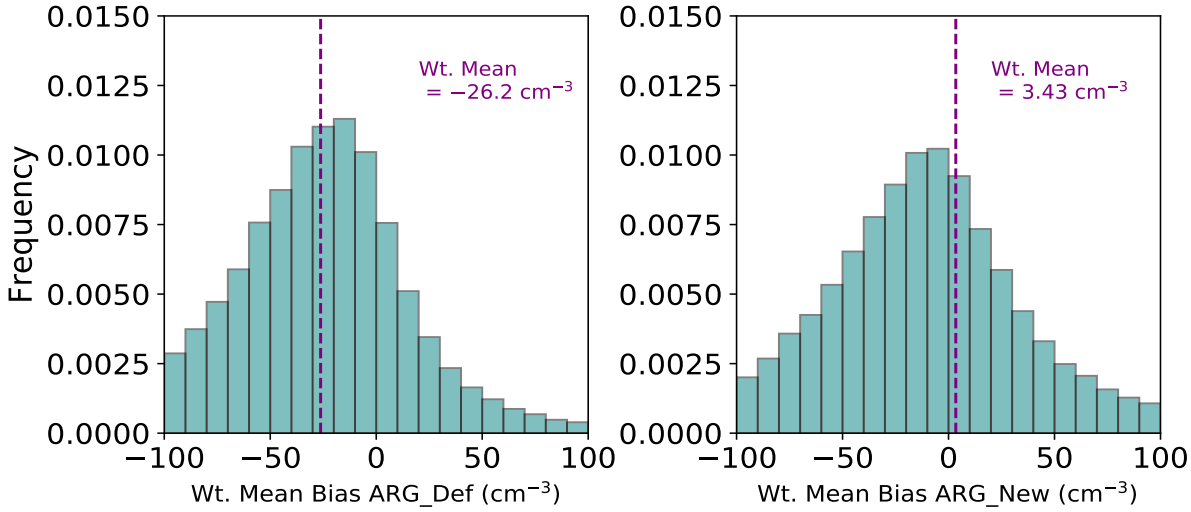

Figure S7. Histograms of mean bias (cm^{-3}) in annual average top-of-cloud daytime droplet concentrations for default (left panel) and updated new ARG scheme (right panel), from the UM simulations are shown.

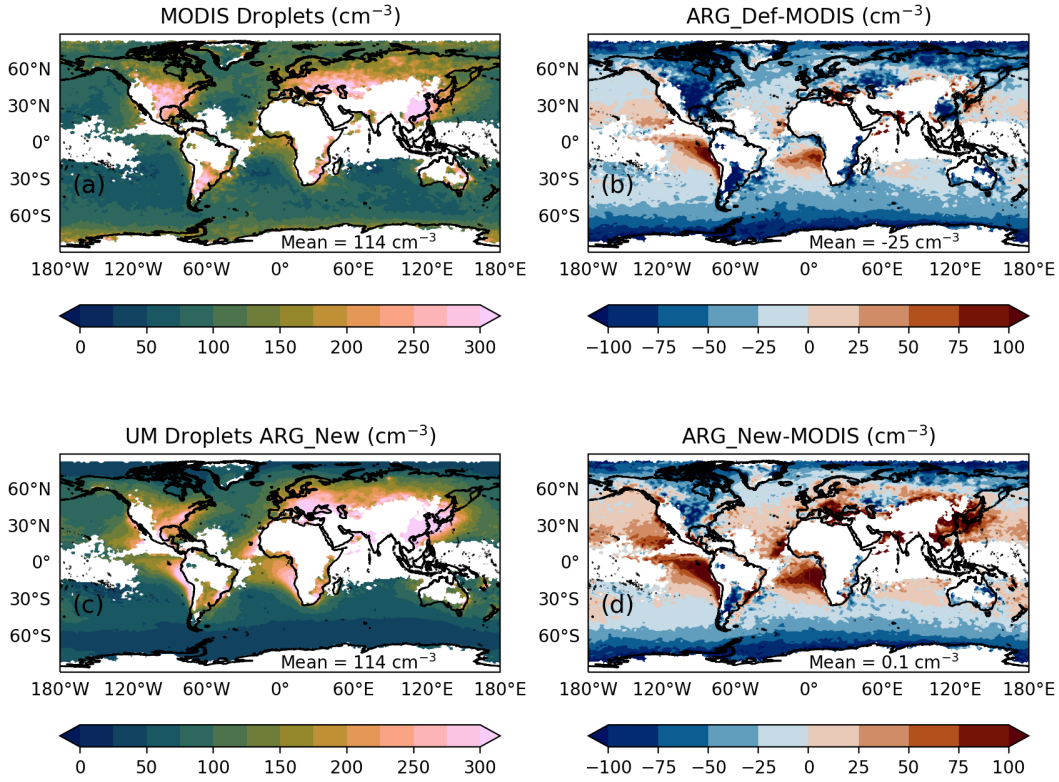

Figure S8. (a) Daytime top-of-cloud droplet number concentrations from MODerate Imaging Spectroradiometer (MODIS) satellite data (Grosvenor et al., 2018) for the annual average of 2014, regridded to the N96 UM grid. (b) Bias in the UM simulation with the default ARG for the same period. (c) Annual average of daytime top-of-cloud droplet number concentrations from the UM simulation with the updated ARG. (d) Bias in the UM simulation with the updated ARG for the same period. The weight used in the denominator to calculate cloud top N_d is obtained from the model as a monthly average diagnostic. For this Figure, we use this monthly diagnostic to identify the 25th percentile of the weight across the entire domain and exclude grid boxes with weights below this threshold.

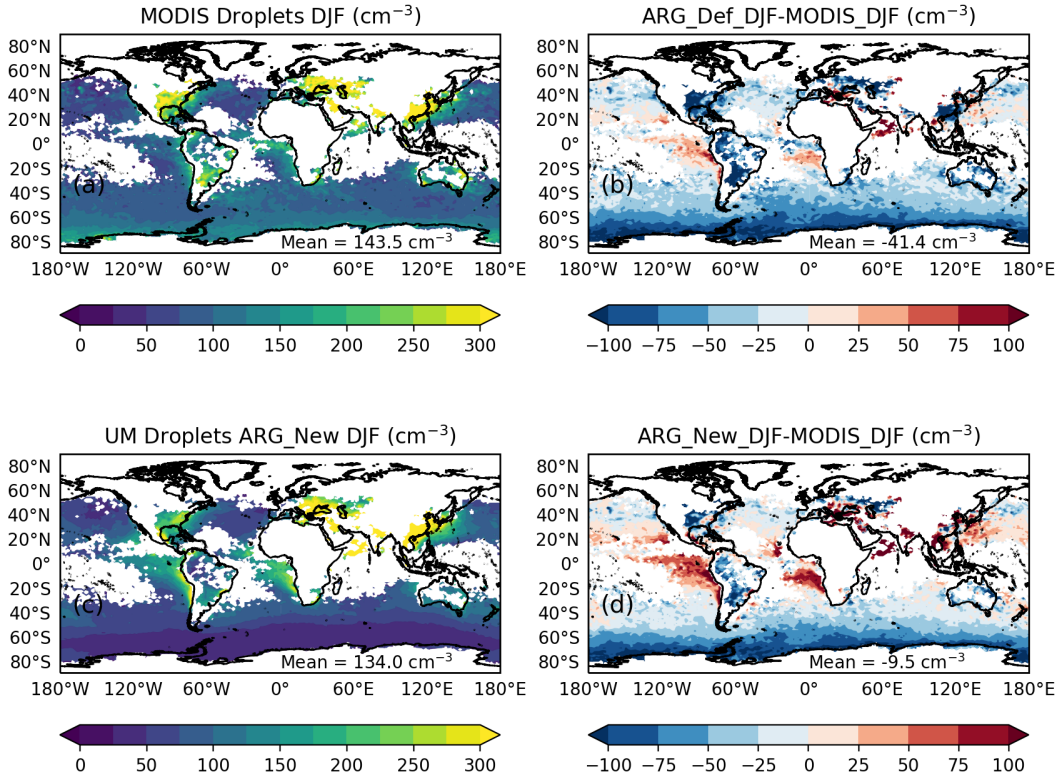

Figure S9. (a) Daytime top-of-cloud droplet number concentrations from MODerate Imaging Spectroradiometer (MODIS) satellite data (Grosvenor et al., 2018) for the December, January, and February average of 2014, regridded to the N96 UM grid. (b) Bias in the UM simulation with the default ARG for the same period. (c) Daytime top-of-cloud droplet number concentrations from the UM simulation with the updated ARG for the same period. (d) Bias in the UM simulation with the updated ARG for the same period.

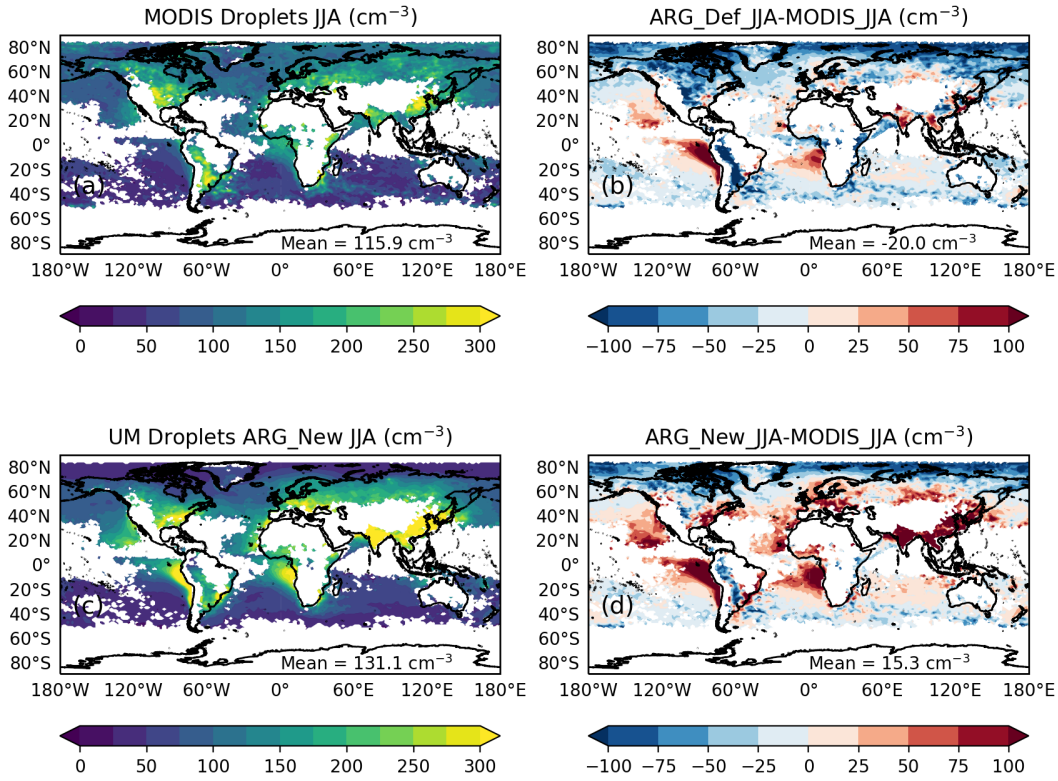

Figure S10. (a) Daytime top-of-cloud droplet number concentrations from MODerate Imaging Spectroradiometer (MODIS) satellite data (Grosvenor et al., 2018) for the June, July, and August average of 2014, regridded to the N96 UM grid. (b) Bias in the UM simulation with the default ARG for the same period. (c) Daytime top-of-cloud droplet number concentrations from the UM simulation with the updated ARG for the same period. (d) Bias in the UM simulation with the updated ARG for the same period.

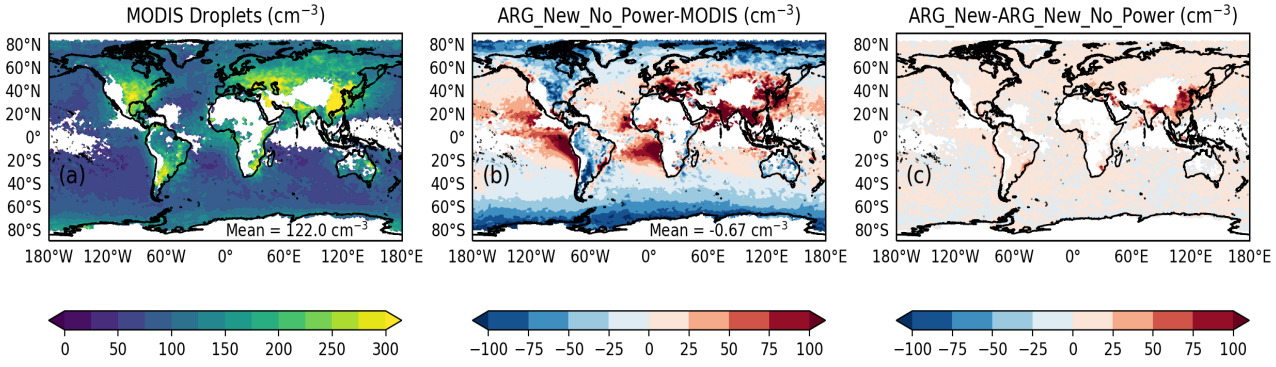

Figure S11. (a) Annual average of daytime top-of-cloud droplet number concentrations from MODerate Imaging Spectroradiometer (MODIS) satellite data (Grosvenor et al., 2018) regridded to the N96 UM grid. (b) Mean bias in UM simulations with updated ARG but without modifications for the kinetic limitations (ARG_New_No_Power). (c) Mean annual difference between the UM simulation with the updated ARG scheme and the updated ARG scheme without the modifications for the high aerosol concentration regions.

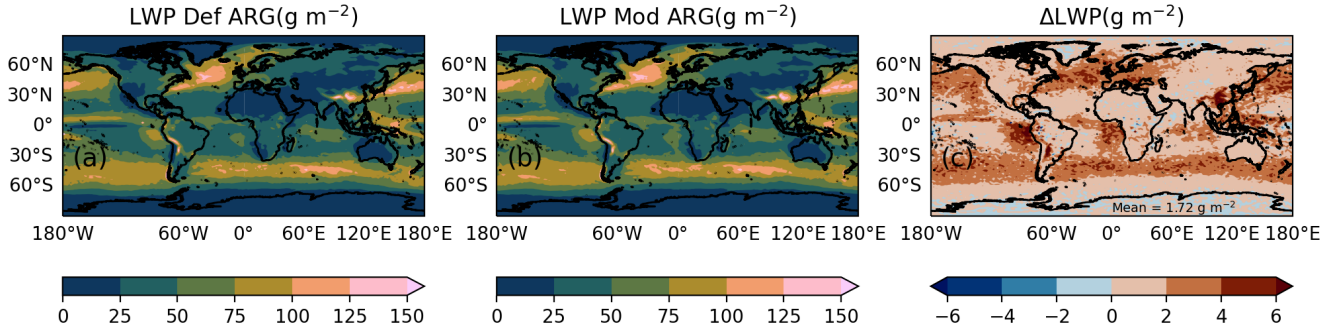

Figure S12. Annual averaged (for 2014) global spatial distribution of liquid water path in present day simulation with default ARG (a), updated ARG (b), and the difference between updated and default simulations (c).

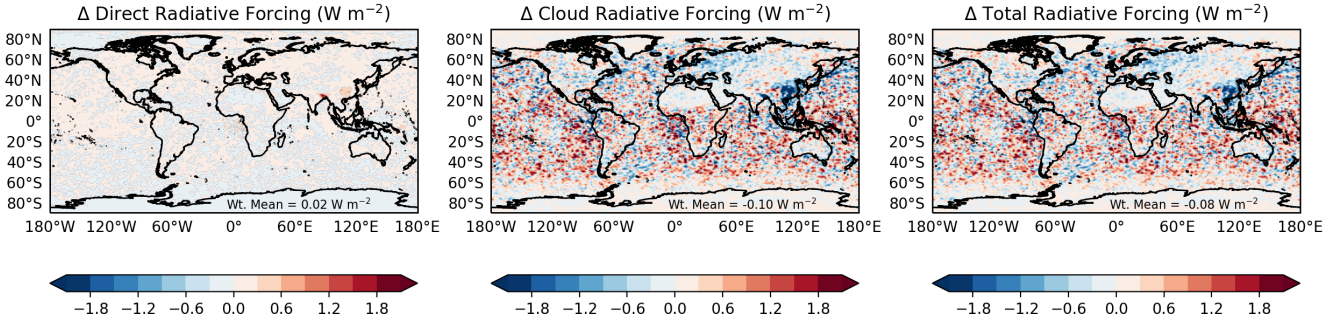

Figure S13. Global spatial distribution of changes in radiative forcing estimates (left, direct, middle, cloud right, total) due to changing the constants used in default ARG, are shown here.

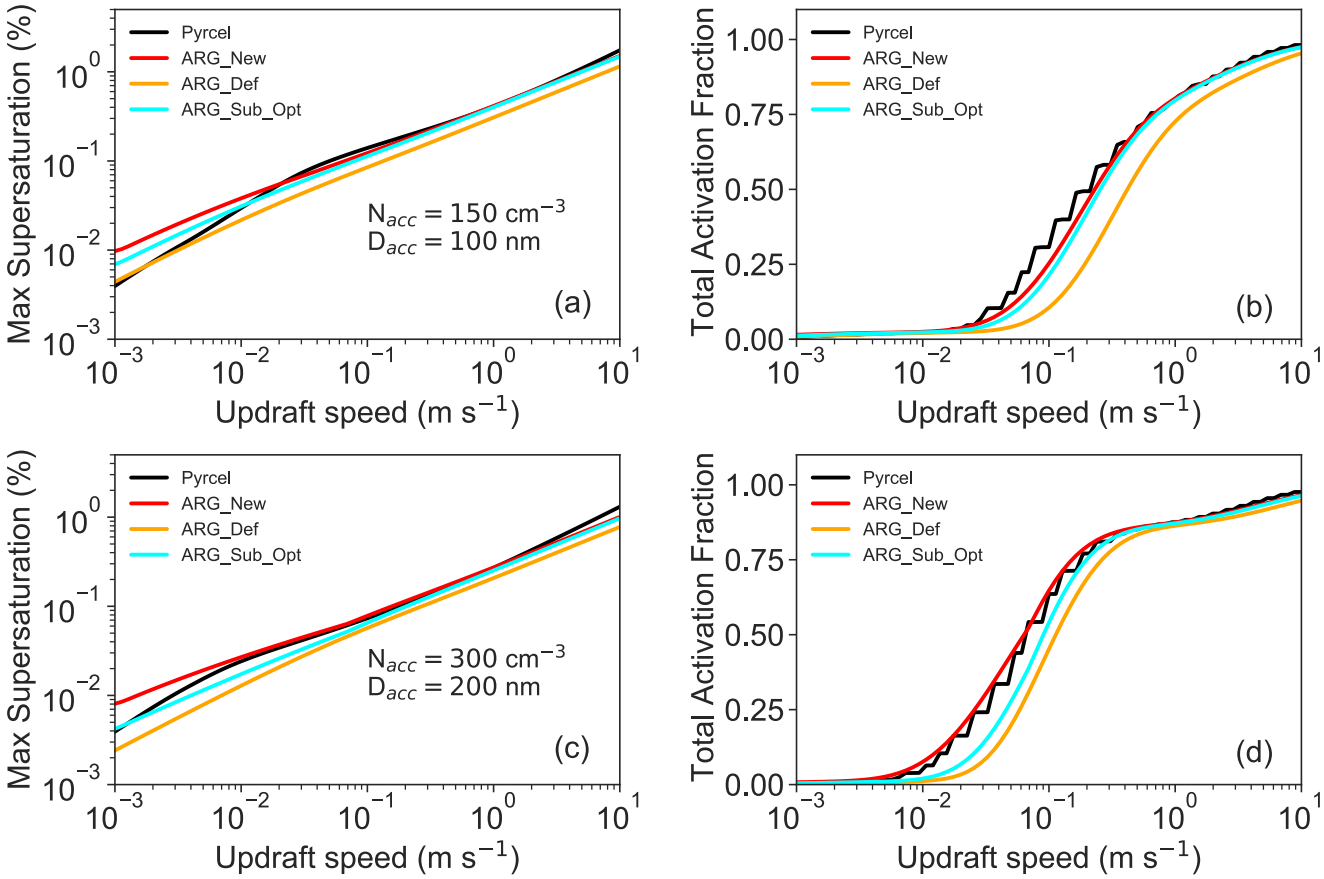

Figure S14. Maximum supersaturation (subfigure a, c) and total activation fraction (subfigure b, d) as a function of updrafts for different aerosol number concentrations. Details of aerosol concentrations are listed in Table S1. Results from parcel model along with default ARG, updated new ARG and our 'sub-optimal ARG' sensitivity study are shown. In the 'sub-optimal' simulation, we set $f = 0.70$, $g = 0.67$, and $p = 1.20$. These parameters underestimate accumulation mode activation fraction 83% of the time in our parameter set.

References

Abdul-Razzak, H. and Ghan, S.: A parameterization of aerosol activation: 2. Multiple aerosol types, Journal of Geophysical Research, 105, 6837–6844, https://doi.org/10.1029/1999JD901161, 2000.

Grosvenor, D. P., Sourdeval, O., Zuidema, P., Ackerman, A., Alexandrov, M. D., Bennartz, R., Boers, R., Cairns, B., Chiu, J. C., Christensen, M., Deneke, H., Diamond, M., Feingold, G., Fridlind, A., Hünerbein, A., Knist, C., Kollias, P., Marshak, A., McCoy, D., Merk, D., Painemal, D., Rausch, J., Rosenfeld, D., Russchenberg, H., Seifert, P., Sinclair, K., Stier, P., van Diedenhoven, B., Wendisch, M., Werner, F., Wood, R., Zhang, Z., and Quaas, J.: Remote Sensing of Droplet Number Concentration in Warm Clouds: A Review of the Current State of Knowledge and Perspectives, Reviews of Geophysics, 56, 409–453, https://doi.org/https://doi.org/10.1029/2017RG000593, 2018.